

# Lawrence Berkeley National Laboratory

## Recent Work

### Title

THE REACTION  $n+p \rightarrow \pi^0 + p$  AT MOMENTA FROM 20 TO 200 GeV/c

### Permalink

<https://escholarship.org/uc/item/4c7579bh>

### Author

Dahl, O.I.

### Publication Date

1976-11-01

Submitted to Physical Review Letters

LBL-5547 c1  
CALT-68-569  
Preprint

THE REACTION  $\pi^-p \rightarrow \omega n$  AT  
MOMENTA FROM 20 TO 200 GeV/c

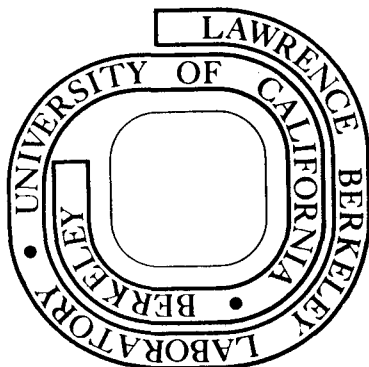
O. I. Dahl, R. A. Johnson, R. W. Kenney, M. Pripstein,  
A. V. Barnes, D. J. Mellema, A. V. Tollestrup, and  
R. L. Walker

November 1976

Prepared for the U. S. Energy Research and  
Development Administration under Contract W-7405-ENG-48

**For Reference**

Not to be taken from this room



LBL-5547  
c1

## **DISCLAIMER**

This document was prepared as an account of work sponsored by the United States Government. While this document is believed to contain correct information, neither the United States Government nor any agency thereof, nor the Regents of the University of California, nor any of their employees, makes any warranty, express or implied, or assumes any legal responsibility for the accuracy, completeness, or usefulness of any information, apparatus, product, or process disclosed, or represents that its use would not infringe privately owned rights. Reference herein to any specific commercial product, process, or service by its trade name, trademark, manufacturer, or otherwise, does not necessarily constitute or imply its endorsement, recommendation, or favoring by the United States Government or any agency thereof, or the Regents of the University of California. The views and opinions of authors expressed herein do not necessarily state or reflect those of the United States Government or any agency thereof or the Regents of the University of California.

THE REACTION  $\pi^- p \rightarrow \omega n$  AT MOMENTA FROM 20 TO 200 GeV/c<sup>\*</sup>O. I. Dahl, R. A. Johnson,<sup>†</sup> R. W. Kenney, and M. PripsteinLawrence Berkeley Laboratory  
Berkeley, California 94720

and

A. V. Barnes, D. J. Mellema,<sup>‡</sup> A. V. Tollestrup, and R. L. WalkerCalifornia Institute of Technology  
Pasadena, California 91125

## ABSTRACT

The reaction  $\pi^- p \rightarrow \omega n$  in the beam momentum range from 20 to 200 GeV/c has been studied using data acquired at Fermilab. In this letter, the integral and differential cross sections for this reaction are presented. The integral cross sections are considerably larger than those previously reported. The differential cross sections can be reproduced quite easily by Regge models. As predicted by such models, natural parity exchange dominates production throughout this energy region.

---

\* Work supported in part by U. S. Energy and Development Administration. Prepared under Contract No. W-7405-ENG-48 at Lawrence Berkeley Laboratory and Contract No. E(11-1)-68 at California Institute of Technology.

† Present address: Brookhaven National Laboratory, Upton, NY 11973

‡ Present address: Hughes Aircraft Co., Culver City, CA 90230

The reaction  $\pi^- p \rightarrow \omega n$  offers a good opportunity to test the Regge formalism for high energy interactions. Two non-interfering mechanisms (natural and unnatural parity exchange) contribute to the production cross section and each of these processes has its own characteristic energy dependence. Furthermore, these two parts can be separated by measuring the final spin-density matrix of the  $\omega$ .

Omega production events (with the decay  $\omega \rightarrow \pi^0 \gamma$ ) were accumulated simultaneously with charge exchange and eta production data in an experiment performed at Fermilab during 1974. A total of 2100 omega events have been found among these data which were taken at six energies from 20 to 200 GeV. The apparatus, methods of data accumulation, and basic analysis schemes are described in reports on the charge exchange and eta production measurements.<sup>1-3</sup>

In the experiment, only a portion of the phase space for omega decay was observed. Therefore, determination of the production spin-density matrix was crucial for extrapolating into the unobserved regions. Finding the decay angles for a given event required complete reconstruction of that event. This involves the complex problem of matching showers seen in one plane of the detector with those in the other. Fortunately, the requirement that a  $\pi^0$  be found in an omega-like event provides an extremely powerful constraint and virtually eliminates all wrong matches.

To reduce geometric effects and to improve mass resolution, cuts were made on the  $\omega$  decay angle ( $|\cos\theta_{\omega \rightarrow \pi^0 \gamma}| < .6$ ) and the  $\pi^0$  decay angle ( $|\cos\theta_{\pi^0 \rightarrow \gamma \gamma}| < .9$ ). The  $\omega$  mass<sup>2</sup>,  $\pi^0$  mass<sup>2</sup>, and  $\omega$  decay angle distributions for the 150 GeV/c data are shown in Fig. 1. The background under the  $\omega$  mass peak varied from 25% at 20 GeV/c to 12% at 200 GeV/c. It is peaked

at extremely small production angles, and its decay is flat in phase space. Both of these facts indicate that the background comes from  $\pi^- p \rightarrow \pi^0 \pi^0 n$  events in which only three photons are recognized.

The helicity-frame spin-density matrix elements are determined for each  $t$  bin by making a maximum likelihood fit of the decay distribution to the functional form

$$W(\theta, \phi) = \frac{3}{8\pi} \left\{ (1 + \cos^2 \theta) - \frac{\rho_{0,0}}{2} (3 \cos^2 \theta - 1) + \rho_{1,-1} \sin^2 \theta \cos 2\phi \right. \quad (1) \\ \left. + \sqrt{2} \operatorname{Re}(\rho_{1,0}) \sin 2\theta \cos \phi \right\}$$

plus a flat background term. Monte Carlo integration techniques were used to determine the average detection efficiency.<sup>4</sup> Different assumptions about the shape of the background change the numerical value of the spin-density matrix slightly, but leave the average detection efficiency virtually constant.

Representative density matrix elements are displayed in Fig. 2a. It is the cosine-like structure in the  $\phi$  distribution (Fig. 1d) that forces the parameter  $\rho_{1,-1}$  to be large and consequently  $\rho_{0,0}$  to be small.<sup>5</sup> At high energies, the combination  $\rho_+ = \rho_{1,1} + \rho_{1,-1}$  ( $\rho_- = \rho_{1,1} - \rho_{1,-1}$ ) projects out only natural (unnatural) parity exchange<sup>6</sup> ( $\rho_{1,1} = \frac{1}{2} - \frac{1}{2} \rho_{0,0}$ ). As can be seen from Fig. 2a, in this energy regime almost the entire cross section comes from natural parity exchange.

The total and differential cross sections for omega production are listed in Table 1. The normalization corrections applied to these data are similar to those discussed in Ref. 3. In Fig. 3, the total cross sections are compared with previous measurements. The discrepancy between the results of this experiment and those of Bolotov, et al.<sup>7</sup> arises from differences in the assumed value of  $\rho_{0,0}$ . If  $\rho_{0,0} = .57$  had been used here as in Ref. 7, the two results would agree; however, this value of  $\rho_{0,0}$  is

inconsistent with our observed  $\phi$  distribution. The change in slope of the total cross sections from the region below 10 GeV/c<sup>8-10</sup> to the region of this experiment is predicted by Regge theory. The unnatural parity exchange portion of the cross section, which is sizeable below 10 GeV/c,<sup>11</sup> is mediated by B-trajectory exchange. This portion is expected to decrease faster with energy than the natural parity part which is mediated by  $\rho$  trajectory exchange. Above 20 GeV/c, the effects of unnatural parity exchange have all but died away and the new slope of the total cross section is less steep.

Also plotted on Fig. 3 is the total eta production cross section.<sup>2,3</sup> Although the agreement of the magnitudes of the eta and omega production cross sections may be coincidental, the similarity in slope again indicates that natural parity exchange now dominates production.

As shown in Fig. 2b, each differential cross section has a dip in the forward direction which is characteristic of  $\rho$  exchange interactions, and a structureless exponential fall past  $t = -.15 \text{ GeV}^2$ . The Regge model predictions which Irving and Michael obtained from 6 GeV/c data<sup>12</sup> are also shown in Fig. 2b. Although the actual dip in the forward direction seems less dramatic than predicted and the high  $t$  cross section falls less rapidly, the agreement between the data and their predictions is quite remarkable. It is clear that a similar Regge model can accurately reproduce all features of both these and the lower energy cross sections.

As indicated before, the natural parity exchange dominates most of the production cross section. Fits of the differential cross sections to the form

$$d\sigma/dt = A(t) p_{\text{beam}}^{2\alpha(t)-2} \quad (2)$$

confirm this observation; the values  $\alpha(t)$  lie almost on top of the

$\rho$ -trajectory obtained from pion charge exchange<sup>1</sup> (Fig. 4). Only in the forward direction is there appreciable departure from this trajectory. In that direction, the  $\rho$  residue function goes to zero and processes involving lower-lying unnatural parity trajectories are emphasized. Therefore, a departure of the effective trajectory from that of the  $\rho$  is expected.



Footnotes

1. A. V. Barnes, et al., Phys. Rev. Lett. 37, 76 (1976).
2. O. I. Dahl, et al., Phys. Rev. Lett. 37, 80 (1976)
3. R. A. Johnson, thesis, Lawrence Berkeley Laboratory Report, LBL-4610 (unpublished).
4. Details of the omega selection criteria and the spin-density matrix fit can be found in R. A. Johnson, Lawrence Berkeley Laboratory Report, LBL-5548 (unpublished).
5. The requirement that the spin-density matrix is positive-definite leads to the constraint  $|\rho_{1,-1}| \leq \rho_{1,1}$  where  $\rho_{1,1} = \frac{1}{2} - \frac{1}{2} \rho_{0,0}$ .
6. G. Cohen-Tannoudji, et al., Nuovo Cimento, 55A, 412 (1968);  
J. P. Adler, et al., Nuovo Cimento 56A, 952 (1968).
7. V. N. Bolotov, et al., Phys. Lett. 53B, 217 (1968).
8. E. Shibata and M. A. Wahlig, Phys. Lett. 22, 354 (1966).
9. L. E. Halloway, et al., Phys. Rev. D8, 2814 (1973).
10. W. D. Apel, et al., Phys. Lett. 55B, 111 (1975).
11. See for example; M. H. Shaevitz, et al., Phys. Rev. Lett. 36, 8 (1976).
12. A. C. Irving and C. Michael, Nuc. Phys. B82, 282 (1974).
13. Particle Data Group, Rev. of Mod. Phys. 48, S1 (1976).

### Captions

Table 1. Differential cross section in  $\mu\text{b}/\text{GeV}^2$  and other results from the reaction  $\pi^- p \rightarrow \omega n$  with the decay  $\omega \rightarrow \pi^0 \gamma$ . The differential cross sections are averages over the  $t$ -interval; no finite bin width corrections have been made. Errors are only statistical; the overall normalization error is 10%. The right-hand column contains the effective Regge trajectory obtained by fitting the data to the parameterization of equation (2).

Figure 1. (a) The 150 GeV/c three-photon mass<sup>2</sup> spectrum of events surviving all cuts except that for mass<sup>2</sup>; (b) the mass<sup>2</sup> spectrum of the two photons assumed to be the  $\pi^0$ ; (c) the helicity-frame polar angle distribution for  $\omega$ -like events; and (d) the azimuthal angle distribution. The events in the region labeled BG in (a) were used to determine the properties of the background; events between these sections were assumed to be  $\omega$ s. In (c) and (d), the solid line represents the  $\omega$  and background events from the  $\omega$  mass region and the dotted line represents background events from the BG regions.

Figure 2. (a) Representative spin-density matrix elements; and (b) representative differential cross sections. The dashed lines in (b) are the predictions of Irving and Michael<sup>12</sup> which are based on 6 GeV/c data.

Figure 3. The total  $\omega$  production cross section. Data from Refs. 7-10 are plotted. The partial fraction of the  $\omega \rightarrow \pi^0 \gamma$  decay mode is taken to be 8.8%.<sup>13</sup>

Figure 4. The effective Regge trajectory. The  $\rho$ -trajectory is taken from Ref. 1 and the B-trajectory is the one assumed in Ref. 12.

-t Bin GeV <sup>2</sup>	Beam Momentum in GeV						$\alpha(t)$
	20.8	40.8	64.4	100.7	150.2	199.3	
0.00 - 0.05	1.8 ± 0.7	0.72 ± 0.19	0.43 ± 0.17	0.21 ± 0.05	0.12 ± 0.03	0.024 ± 0.016	0.18 ± 0.07
0.05 - 0.10	1.9 ± 0.5	0.74 ± 0.21	0.54 ± 0.10	0.25 ± 0.04	0.20 ± 0.04	0.082 ± 0.016	0.32 ± 0.05
0.10 - 0.15	2.7 ± 0.4	1.13 ± 0.17	0.69 ± 0.09	0.38 ± 0.06	0.20 ± 0.03	0.154 ± 0.023	0.36 ± 0.04
0.15 - 0.20	2.2 ± 0.4	0.98 ± 0.15	0.45 ± 0.10	0.34 ± 0.05	0.17 ± 0.03	0.111 ± 0.019	0.35 ± 0.04
0.20 - 0.25	1.7 ± 0.4	0.62 ± 0.14	0.32 ± 0.06	0.23 ± 0.04	0.10 ± 0.02	0.088 ± 0.018	0.35 ± 0.06
0.25 - 0.30	1.1 ± 0.3	0.48 ± 0.14	0.35 ± 0.06	0.14 ± 0.05	0.10 ± 0.02	0.032 ± 0.012	0.28 ± 0.06
0.30 - 0.40	0.9 ± 0.2	0.31 ± 0.06	0.12 ± 0.03	0.07 ± 0.02	0.026 ± 0.009	0.010 ± 0.004	0.07 ± 0.05
0.40 - 0.50	0.5 ± 0.2	0.17 ± 0.04	0.08 ± 0.03	0.012 ± 0.006	0.019 ± 0.006	0.004 ± 0.003	-0.08 ± 0.11
$\sigma = \int_{-0.5}^0 \frac{d\sigma}{dt} dt$	0.71 ± 0.06	0.28 ± 0.02	0.159 ± 0.013	0.086 ± 0.006	0.049 ± 0.004	0.026 ± 0.002	
Number of events *	437 ± 29	392 ± 25	407 ± 23	383 ± 22	290 ± 19	194 ± 16	

\* after background subtraction

Table 1

00004603887

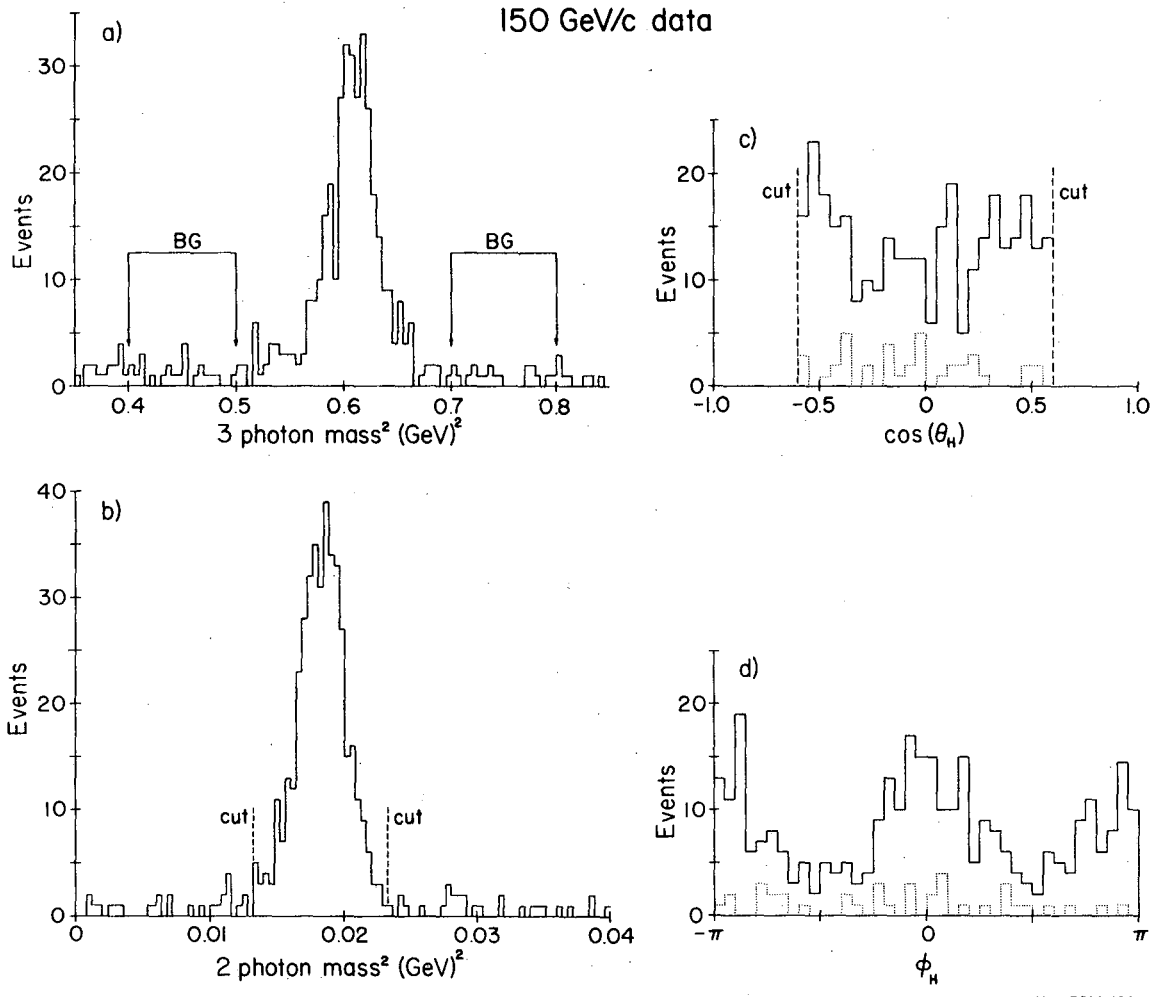
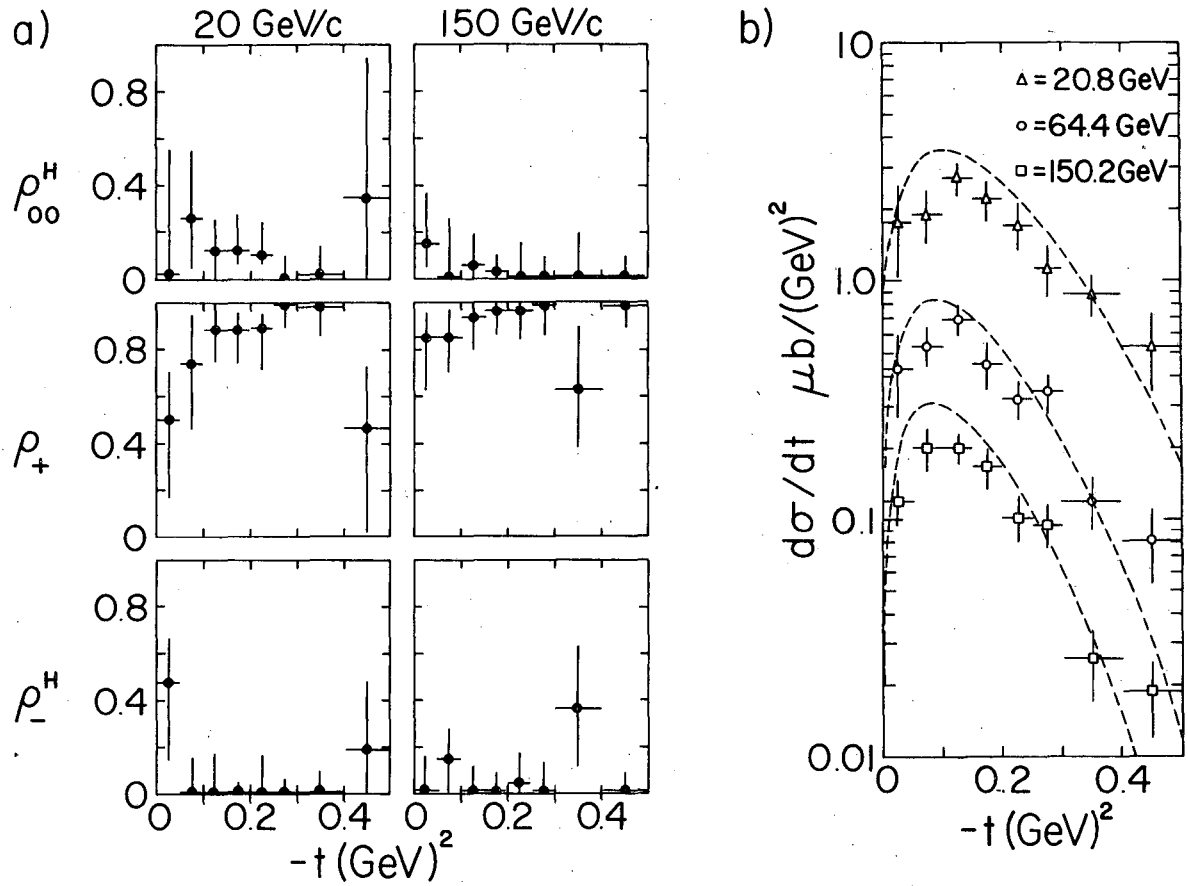
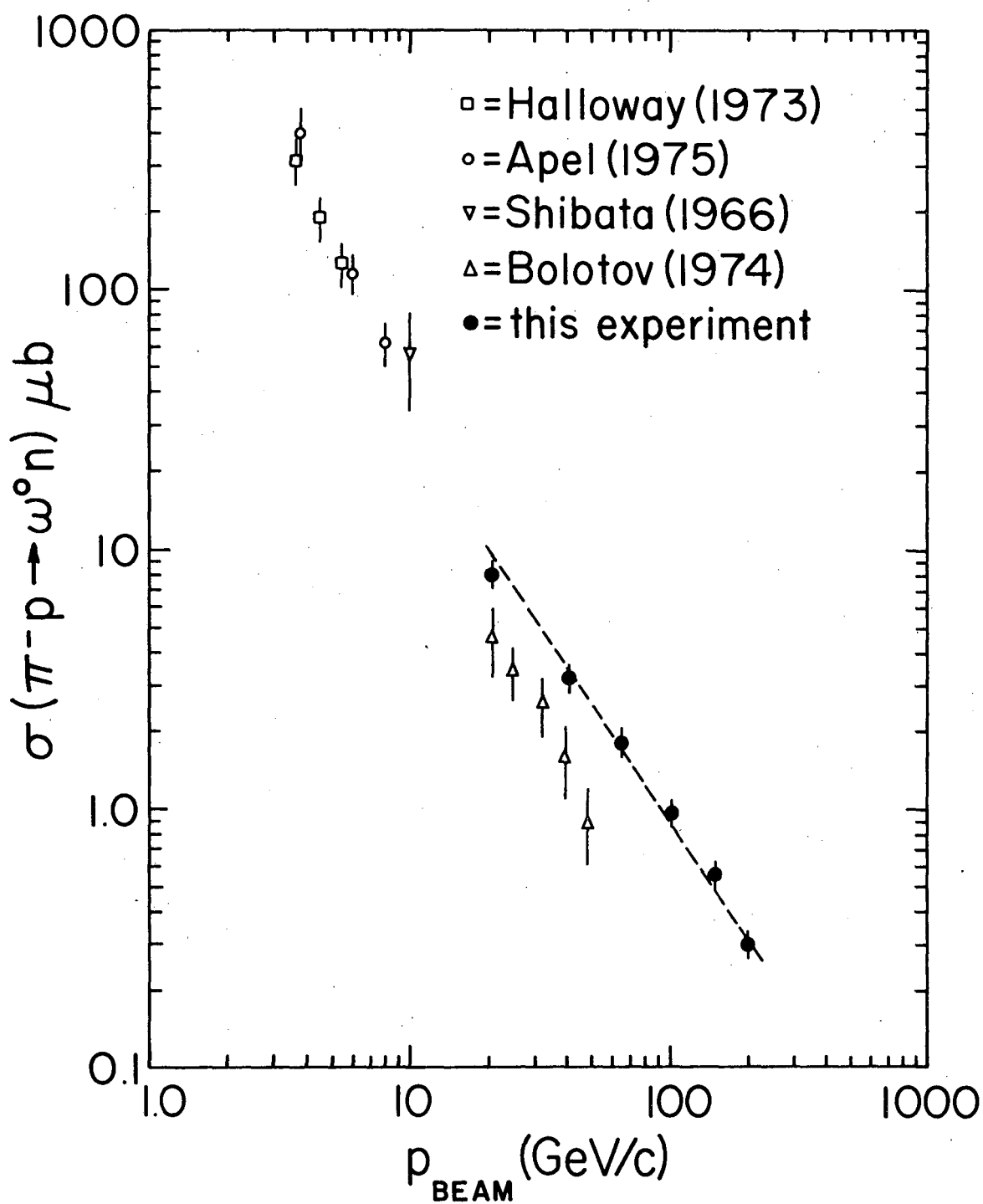


Figure 1



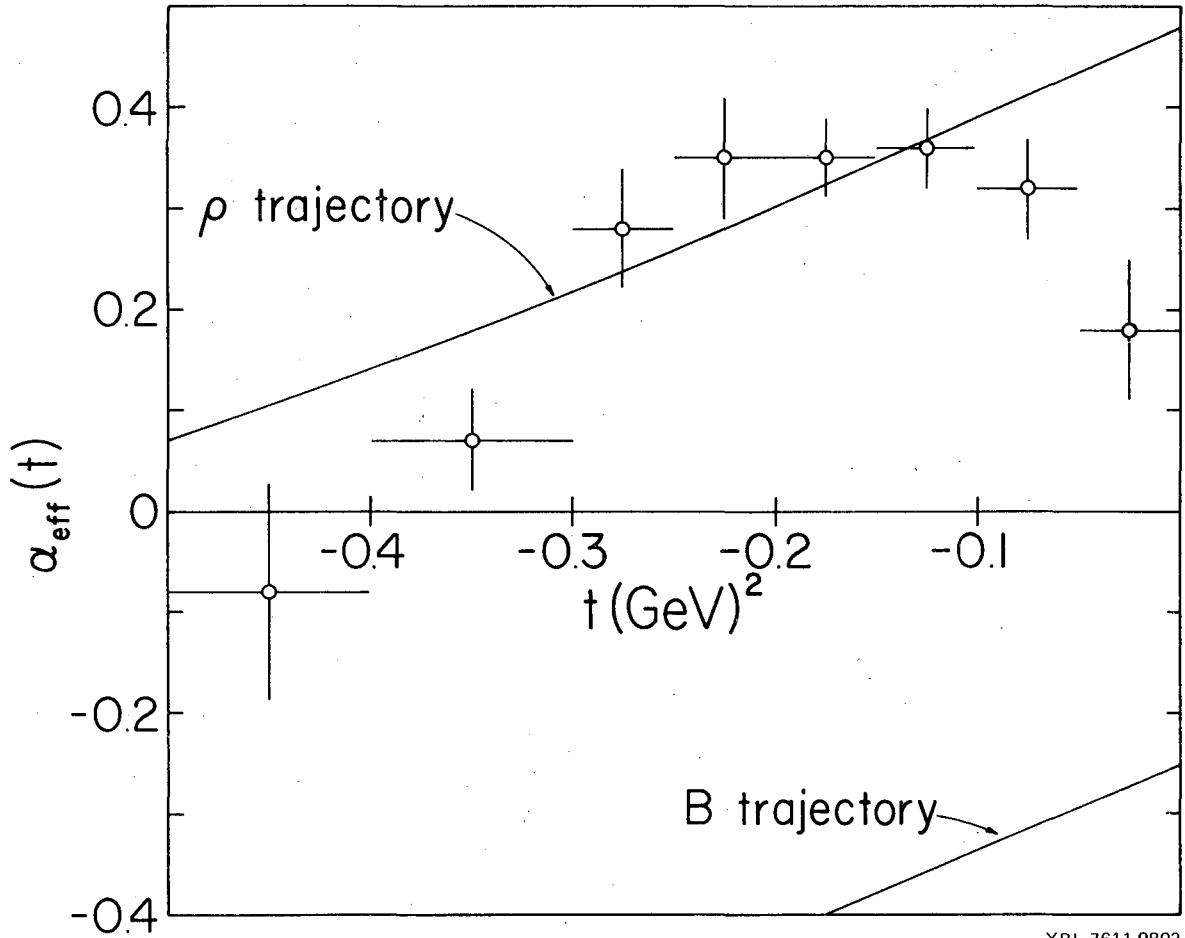
XBL 7610-4645

Figure 2



XBL 7610-4648

Figure 3



XBL 7611-9802

Figure 4

This report was done with support from the United States Energy Research and Development Administration. Any conclusions or opinions expressed in this report represent solely those of the author(s) and not necessarily those of The Regents of the University of California, the Lawrence Berkeley Laboratory or the United States Energy Research and Development Administration.



TECHNICAL INFORMATION DIVISION  
LAWRENCE BERKELEY LABORATORY  
UNIVERSITY OF CALIFORNIA  
BERKELEY, CALIFORNIA 94720